Manuscript submitted to
AIMS' Journals
Volume **00**, Number **0**, Xxxx **XXXX**

doi:

pp. **000–000**

ANISOTROPY IN WAVELET-BASED PHASE FIELD MODELS

Maciek Korzec

Technische Universität Berlin, Institute of Mathematics,
Straße des 17. Juni 136,
10623 Berlin, Germany

Andreas Münch and Endre Süli

Mathematical Institute, University of Oxford,
Andrew Wiles Building, Radcliffe Observatory Quarter, Woodstock Road,
Oxford OX2 6GG, UK

Barbara Wagner*

Weierstrass Institute,
Mohrenstraße 39
10117 Berlin, Germany
and
Technische Universität Berlin, Institute of Mathematics,
Straße des 17. Juni 136,
10623 Berlin, Germany

Abstract. When describing the anisotropic evolution of microstructures in solids using phase-field models, the anisotropy of the crystalline phases is usually introduced into the interfacial energy by directional dependencies of the gradient energy coefficients. We consider an alternative approach based on a wavelet analogue of the Laplace operator that is intrinsically anisotropic and linear. The paper focuses on the classical coupled temperature/Ginzburg–Landau type phase-field model for dendritic growth. For the model based on the wavelet analogue, existence, uniqueness and continuous dependence on initial data are proved for weak solutions. Numerical studies of the wavelet based phase-field model show dendritic growth similar to the results obtained for classical phase-field models.

1. **Introduction.** Since at least the late 1980s, wavelets have been the focus of intensive research and have developed into an indispensable tool for signal and image processing. Wavelet compression is used, for example, in the JPEG2000 image compression standard. From the vast literature on the mathematical theory of wavelets we mention only the ten lectures by Daubechies [8], which provide a classical introduction to the field, and a more recent overview by Mallat [20]. Wavelets have also been explored for their use in numerical approximation of partial

2010 *Mathematics Subject Classification.* Primary: 34E13, 74N20; Secondary: 74E10.

Key words and phrases. Phase-field model, wavelets, sharp interface model, free boundaries.

The first author acknowledges the support by the DFG Matheon research centre, within the project C10, SENBWF in the framework of the program *Spitzenforschung und Innovation in den Neuen Ländern*, Grant Number 03IS2151 and KAUST, award No. KUK-C1-013-04, and the hospitality of the Mathematical Institute at the University of Oxford during his Visiting Postdoctoral Fellowship.

* Corresponding author: Barbara Wagner.

differential equations and operator equations [7] through Galerkin type methods [15], in wavelet collocation methods [30, 29] or as a tool to determine sparse grids for other common discretization methods [16, 14, 6, 27].

A completely new role of wavelets in the context of partial differential equations has recently been introduced by Dobrosotskaya and Bertozzi [9, 10, 11] in applications from image processing. The key idea is to replace the Laplace operator in a Ginzburg–Landau free energy formulation by a pseudo-differential operator defined in wavelet space, by using a Besov type seminorm instead of the standard Sobolev H^1 seminorm. In the Euler–Lagrange equation the Laplacian is correspondingly replaced by a "derivative-free" wavelet analogue. The new approach, intended to improve results for sharper image reconstructions, also introduced anisotropy of the solutions with a four- or eight-fold symmetry. In particular, the authors determined and proved the Γ-limit for the new energy [10, 2], showed the square anisotropy of the Wulff shape [33, 13, 4], and proved the well-posedness of the wavelet analogue of the Allen–Cahn equation [11]. In the work presented here, we make use of this idea to model anisotropic patterns in dendritic growth.

One of the most widely studied model equations of dendritic recrystallization goes back to the work by Kobayashi [18], and has subsequently been discussed in a number of studies, see for example Caginalp [5], Penrose and Fife [26], Wang et al. [31] and McFadden et al. [22]. For reviews we refer to Glicksman [12], Steinbach [28] and, for a survey from an analytical point of view, to the recent review by Miranville [23].

The approach introduces a phase-field model where the gradient terms have an anisotropic weight γ that depends on the direction of the spatial gradient of the phase-field variable ∇u. Usually, γ is written as a function of the angle θ between the direction of ∇u and a reference direction. A typical choice is $\gamma(\theta) = 1+\delta\cos(n\theta)$, where $n > 0$ is an integer parameter that leads to an n-fold symmetry and $\delta \geq 0$ denotes the strength of the anisotropy.

For this type of anisotropic recrystallization model, existence of solutions has been shown in Burman and Rappaz [3]. To correctly capture the interfacial instability various numerical methods have been developed, starting with Kobayashi's own work [18], or for example in Wheeler et al. [32], Karma and Rappel [17], McFadden [21], Li et al. [19] and more recently in Barrett et al. [1], who also gave an overview of various numerical approaches to phase-field models and their associated sharp interface limits.

In this study we present a new anisotropic recrystallization model, where the leading derivative of the phase field variable is replaced by a wavelet analogue, and we show that it captures dendritic growth that is similar to the classical recrystallization model. However, while Kobayashi's classical model is quasilinear in the phase field variable, the new model does not contain spatial derivatives of the phase field variable. Moreover, the new wavelet term is linear and has a simple form in wavelet space, very similar to the diagonal representation of differential operators in Fourier space. As a consequence, the mathematical analysis and the numerical approximation of the new system of partial differential equations simplify greatly.

The paper is structured as follows. We begin with a formulation of both models in Section 2, where we also summarize the essential notions about wavelets and Besov-type norms, and we introduce a wavelet analogue of the Laplacian. In Section 3, we prove well-posedness, in particular we show the existence and uniqueness of solutions. Results from numerical experiments that explore the anisotropic evolution

of these models and comparisons with classical models are discussed in Section 4. Starting with a simpler, limiting case, the anisotropic Allen–Cahn equation, we first investigate the different scaling behaviors of the evolution of the original anisotropic Allen–Cahn equation and its wavelet analogue. Then for the full recrystallization model the dendritic morphologies are discussed. Finally, in Section 5, we summarize our results and their implications and give an outlook on further directions of research.

2. Dendritic recrystallization: two approaches to anisotropy.

2.1. Kobayashi's classical anisotropic model.

In one of the first studies to describe the growth of dendrites from a melt similar to the one observed in experiments, Kobayashi [18] introduced a model that couples an anisotropic evolution equation for a phase field describing the melt-solid transition with an equation for the heat generation and diffusion. The phase-field u is 0 in the liquid and 1 in the solid phase, and the temperature field is denoted by T. Both are assumed to be functions on the 2-dimensional unit box, $\Omega := (0,1)^d$ with $d = 2$, which are 1-periodic in both spatial co-ordinate directions. The evolution of the phase-field is obtained from the $L^2(\Omega)$ gradient flow

$$\tau\, u_t = -\frac{\delta \mathcal{E}}{\delta u} \tag{1}$$

of the Ginzburg–Landau type free energy

$$\mathcal{E} = \mathcal{E}(u;\varepsilon,m) = \int_\Omega \frac{\varepsilon}{2}\gamma(\theta)^2\,|\nabla u|^2 + \frac{1}{\varepsilon}W(u;m)\,\mathrm{d}x, \tag{2}$$

with the interface energy

$$\gamma(\theta) = 1 + \delta\cos(n\theta), \tag{3}$$

for an anisotropy with an n-fold symmetry and strength $\delta \geq 0$, and the homogeneous free energy contribution

$$W(u;m) = \frac{1}{4}u^2(u-1)^2 + m\left(\frac{1}{3}u^3 - \frac{1}{2}u^2\right). \tag{4}$$

The positive parameter $\varepsilon \ll 1$ in (2) controls the width of the interface layer and the parameter $\tau > 0$ in (1) is a relaxation constant. For $x = (x_1, x_2) \in \Omega := (0,1)^2$, the angle θ is defined as $\theta = \arctan\left(u_{x_1}/u_{x_2}\right)$. For an isotropic system, $\gamma(\theta)$ is a constant, while in this study we consider weak anisotropies with a four-fold symmetry by choosing $n = 4$ and a positive δ so that $\gamma(\theta) + \gamma''(\theta)$ (with $' = \mathrm{d}/\mathrm{d}\theta$) is strictly positive for all θ (i.e. $\delta \in (0, 1/15)$).

Thus, we have the Ginzburg–Landau type equation

$$\tau\, u_t = \varepsilon\left[\nabla\cdot\left(\gamma(\theta)\gamma'(\theta)\,\nabla^\perp u\right) + \nabla\cdot\left(\gamma(\theta)^2\,\nabla u\right)\right] + \frac{1}{\varepsilon}W'(u;m), \tag{5}$$

where $\nabla^\perp u := (-u_{x_2},\, u_{x_1})^{\mathrm{T}}$ is the orthogonal gradient.

This equation is coupled to the equation for the temperature T by the latent heat contribution arising from the phase change at the interface via

$$T_t = c\,\Delta T + K u_t, \tag{6}$$

where c is the thermal diffusivity and K is the latent heat, and via the time dependence of m,

$$m(T) = \frac{c_1}{\pi}\arctan\left(c_2\,(T_e - T)\right), \tag{7}$$

where T_e denotes the dimensionless equilibrium (or melting) temperature. We will typically assume that the scaling for the temperature has been chosen so that $T_e = 1$. Notice that W and m together with the constants c_1 and c_2 need to be carefully chosen so that the function W is always a double-well potential with minima occurring at $u = 0$ and $u = 1$ for $c_1 < 1$, so that spatially homogeneous liquid and solid phases are in equilibrium.

2.2. **Anisotropy in wavelet-based models.** To prepare for the derivation of the wavelet-based model, first recall that for the isotropic case, the free energy functional (2) can be written as

$$\mathcal{E}(u;\zeta,\varepsilon,m) = \frac{\varepsilon}{2}|u|_\zeta^2 + \int_\Omega \frac{1}{\varepsilon} W(u;m)\,\mathrm{d}x, \tag{8}$$

with the $H^1(\Omega)$ seminorm $|\cdot|_\zeta = |\cdot|_{H^1(\Omega)}$, where the Sobolev space H^m is defined as usual and has the inner product and associated norm

$$(u,v)_{H^m(\Omega)} = \sum_{|l|\le m} \int_\Omega D^l u(x)\, D^l v(x)\,\mathrm{d}x, \quad \|u\|_{H^m(\Omega)} = \sqrt{(u,u)_{H^m(\Omega)}},$$

in multi-index notation. In the case of Sobolev spaces of 1-periodic functions on $\Omega = (0,1)^d$ we shall write $H^m_p(\Omega)$ instead of $H^m(\Omega)$. In the general, anisotropic case, we can also write $\mathcal{E}$ as in (8) with $|u|_\zeta^2 = |u|_A^2$, where

$$|u|_A^2 = \int_\Omega \gamma(\theta)^2 |\nabla u|^2\,\mathrm{d}x, \tag{9}$$

but $|\cdot|_A$ is not in general a seminorm, as θ depends on the derivatives of u. We now follow Dobrosotskaya and Bertozzi in [9, 10, 11], and introduce a new seminorm $|\cdot|_B$, which gives rise to an anisotropic evolution.

We begin by considering a class of wavelets $\psi \in L^2(\mathbb{R}^d)$ with an associated scaling function $\phi \in L^2(\mathbb{R}^d)$. We define the wavelet mode (j,k) as

$$\psi_{j,k}(x) = 2^{jd/2}\psi(2^j x - k), \quad j = 0,1,2,\ldots;\ k \in \mathbb{R}^d,$$

and the wavelet transform of a function $u \in L^2(\mathbb{R}^d)$ at the mode (j,k) is defined by

$$w_{j,k} = \langle u, \psi_{j,k}\rangle,$$

where $\langle\cdot,\cdot\rangle$ denotes the inner product in $L^2(\mathbb{R}^d)$. Analogously, we define

$$\phi_{j,k}(x) = 2^{jd/2}\phi(2^j x - k), \quad j = 0,1,2,\ldots;\ k \in \mathbb{R}^d.$$

For any function $u \in L^2(\mathbb{R}^d)$, we define the seminorm

$$|u|_B = \left(\sum_{j=0}^{\infty} 2^{2j} \int_{\mathbb{R}^d} |\langle u, \psi_{j,k}\rangle|^2\,\mathrm{d}k\right)^{\frac{1}{2}}.$$

The wavelet Laplacian of $u \in L^2(\mathbb{R}^d)$ is formally defined as

$$\Delta_w u(x) = -\sum_{j=0}^{\infty} 2^{2j} \int_{\mathbb{R}^d} \langle u, \psi_{j,k}\rangle \psi_{j,k}(x)\,\mathrm{d}k.$$

A simple (but lengthy) calculation based on Fourier transforms shows that, for sufficiently regular functions u and v defined on $\mathbb{R}^d$, and any d-component multi-index α, one has

$$\begin{aligned}\langle -\Delta_w u, D^\alpha v\rangle &= \int_{\mathbb{R}^d} (-\Delta_w u)^\wedge(\xi)\,(-\imath\xi)^\alpha\,\overline{\hat v(\xi)}\,\mathrm{d}\xi \\ &= (-1)^{|\alpha|}\int_{\mathbb{R}^d} (\imath\xi)^\alpha \hat u(\xi)\sum_{j=0}^\infty 2^{2j}|\hat\psi(2^{-j}\xi)|^2\,\overline{\hat v(\xi)}\,\mathrm{d}\xi = (-1)^{|\alpha|}\langle -\Delta_w D^\alpha u, v\rangle.\end{aligned}$$

Thus, for any multi-index α, the wavelet Laplacian Δ_w and the differential operator D^α commute. In particular, for $\alpha = 0$ and $v = u$,

$$\begin{aligned}\langle -\Delta_w u, u\rangle &= \int_{\mathbb{R}^d} |\hat u(\xi)|^2 \sum_{j=0}^\infty 2^{2j}|\hat\psi(2^{-j}\xi)|^2\,\mathrm{d}\xi = \sum_{j=0}^\infty 2^{2j}\int_{\mathbb{R}^d} |\hat u(\xi)\,\hat\psi(2^{-j}\xi)|^2\,\mathrm{d}\xi \\ &= \sum_{j=0}^\infty 2^{2j}\int_{\mathbb{R}^d} |F^{-1}(\hat u(\cdot)\,\hat\psi(2^{-j}\cdot))(\kappa)|^2\,\mathrm{d}\kappa \\ &= \sum_{j=0}^\infty 2^{2j}\int_{\mathbb{R}^d} |2^{-jd/2}F^{-1}(\hat u(\cdot)\,\hat\psi(2^{-j}\cdot))(2^{-j}k)|^2\,\mathrm{d}k \\ &= \sum_{j=0}^\infty 2^{2j}\int_{\mathbb{R}^d} |\langle u,\psi_{j,k}\rangle|^2\,\mathrm{d}\kappa = |u|_B^2,\end{aligned}$$

where in the transition to the penultimate term in this chain of equalities we used that

$$\begin{aligned}\langle u,\psi_{jk}\rangle = \langle \hat u, \widehat{\psi_{jk}}\rangle &= 2^{-jd/2}\int_{\mathbb{R}^d} \hat u(\xi)\hat\psi(2^{-j}\xi)\,\mathrm{e}^{2\pi\imath(2^{-j}k)\cdot\xi}\,\mathrm{d}\xi \\ &= 2^{-jd/2}F^{-1}(\hat u(\cdot)\,\hat\psi(2^{-j}\cdot))(2^{-j}k).\end{aligned}$$

Next we define an anisotropic counterpart of $|\cdot|_B$. We shall confine ourselves to the case of $d = 2$ dimensions; for $d = 3$, the construction is similar and is therefore omitted. Given a univariate wavelet $\psi \in L^2(\mathbb{R})$ with associated scaling function $\phi \in L^2(\mathbb{R}^d)$, we consider the 'diagonal', 'vertical' and 'horizontal' wavelet functions

$$\psi^d(x_1,x_2) = \psi(x_1)\,\psi(x_2),\ \psi^v(x_1,x_2) = \psi(x_1)\,\phi(x_2),\ \psi^h(x_1,x_2) = \phi(x_1)\,\psi(x_2),$$

and we let $\tilde\Psi = \{\psi^d,\psi^v,\psi^h\}$. With a slight abuse of notation we consider the bivariate scaling function

$$\phi(x_1,x_2) = \phi(x_1)\,\phi(x_2),$$

and we define $\Psi = \tilde\Psi \cup \{\phi\}$.

With $j = 0,1,2,\ldots$, $k \in \mathbb{R}^2$, $x = (x_1,x_2) \in \mathbb{R}^2$, $\psi \in \tilde\Psi$, one scales and dilates to get the modes

$$\psi_{j,k}(x) = 2^j\psi(2^j x - k), \quad \psi \in \tilde\Psi.$$

The corresponding wavelet transform is defined by

$$w_{j,k,\psi} = \int_{\mathbb{R}^2} u(x)\,\psi_{j,k}(x)\,\mathrm{d}x, \quad \psi \in \tilde\Psi. \tag{10}$$

On the bounded domain $\Omega = (0,1)^2$ one uses $j = 0,1,2,\ldots$ and $k \in [0,2^j]^2$, since the spatial shifts only make sense when the supports of the wavelets are contained

in Ω. The wavelet Laplace operator acting on a 1-periodic function $u \in L^2_p(\Omega)$ is then defined by

$$\Delta_w u = -\sum_{\psi\in\tilde{\Psi}} \sum_{j=0}^{\infty} 2^{2j} \int_{k\in[0,2^j]^2} (u,\psi_{j,k})\psi_{j,k}\,\mathrm{d}k, \tag{11}$$

and we further define the seminorm

$$|u|_B = \left(\sum_{\psi\in\tilde{\Psi}} \sum_{j=0}^{\infty} 2^{2j} \int_{k\in[0,2^j]^2} |(u,\psi_{j,k})|^2\,\mathrm{d}k \right)^{\frac{1}{2}}.$$

As previously, we have that for any, sufficiently smooth, 1-periodic functions u and v,

$$(-\Delta_w u, u) = |u|_B^2 \quad \text{and} \quad (-\Delta_w u, D^\alpha v) = (-1)^{|\alpha|}(-\Delta_w D^\alpha u, v).$$

The seminorm $|\cdot|_B$ is equivalent to the $B^1_{2,2}(\Omega)$ Besov seminorm, whenever the wavelets $\psi_{j,k}$ are twice continuously differentiable with $r \geq 2$ vanishing moments, and to its discretized version, where the integral over $k \in [0,2^j]^2$ is replaced by a finite sum over $k \in \mathbb{Z}^2_j := \mathbb{Z}^2 \cap [0,2^j]^2$.

In order to simplify the notation, when discussing multidimensional cases, we shall use ψ as general notation for the wavelet functions, assuming, wherever needed, summation over all of those.

Note that in numerical implementations one has to treat finite expansions and hence one incorporates the scaling function to represent the mass, similarly as with the zeroth mode in a Fourier expansion; hence we change to the extended set $\Psi = \tilde{\Psi} \cup \{\phi\}$ and write

$$f = \sum_{j=0}^{N} \sum_{k\in\mathbb{Z}^2_j} \sum_{\psi\in\Psi} w_{j,k,\psi}\psi_{j,k},$$

with

$$w_{j,k,\psi} = \langle u, \psi_{j,k}\rangle, \qquad \psi \in \Psi.$$

The $L^2_p(\Omega)$ gradient flow of $\mathcal{E}$ now leads to a new wavelet-based model with a new evolution equation for the phase field,

$$\tau u_t = \varepsilon\Delta_w u - \frac{1}{\varepsilon} W_u(u;m), \tag{12a}$$

where Δ_w is the wavelet analogue (11) of the Laplacian, while the equation for the heat diffusion and generation remains unchanged,

$$T_t = c\Delta T + K u_t. \tag{12b}$$

In order to understand the intrinsic anisotropy in this formulation we recapitulate the main result obtained in [10] for the analysis of the energy (8) with $\zeta = B$ and $m = 0$ (i.e. without temperature dependence) in the limit $\varepsilon \to 0$. For compactly supported wavelets that are r-regular, $r \geq 2$, that is

$$\int_\Omega x^j \psi(x)\,\mathrm{d}x = 0, \qquad j = 0,1,\ldots,r,$$

one can prove the Γ-convergence result $\mathcal{E}^* \xrightarrow{\Gamma} G_\infty = \frac{\sqrt{2}}{3} R(u)|u|_{TV(\Omega)}$, where $|u|_{TV(\Omega)}$ is the total variation functional [10], and where

$$\mathcal{E}^*(u;\varepsilon,B) \equiv \begin{cases} \mathcal{E}(u;\varepsilon,B), & u \in H^1(\Omega), \\ \infty, & u \in BV(\Omega)\setminus H^1(\Omega) \end{cases}$$

is the extension of $\mathcal{E}(u;\varepsilon,B)$ to functions of bounded variation (BV).

In the case of the classical Ginzburg–Landau free energy, (8) with $m = 0$ and $\zeta = H^1(\Omega)$, the factor $R(u)$ is constant and the minima of G_∞ are the characteristic functions of spheres [24]. Here, $R(u)$ is defined as the limit of the quotient of the equivalent norms $R(u) = \lim_{\varepsilon\to 0} |u_\varepsilon|_B/|u_\varepsilon|_{H^1(\Omega)}$, which is unique for all sequences $u^\varepsilon \in H^1_p(\Omega)$ with $u_\varepsilon \to u$ in $L^1_p(\Omega)$ as $\varepsilon \to 0$. One can show that

$$G_\infty(\mathbb{1}_E) = \int_{\partial E} \gamma(n;\psi)\,\mathrm{d}l(x)$$

for characteristic functions $u = \mathbb{1}_E$ of sets $E \subset \mathbb{R}^N$ with finite perimeter. The function γ of the normal at the boundary of E turns out to have just the form (3) with $n = 4$.

3. **Well-posedness of the wavelet based model.** As an important prerequisite for meaningful numerical simulations using the new wavelet-based model, we first prove existence, uniqueness and continuous dependence on initial data for weak solutions of the system (12), with initial conditions $u(x,0) = u_0(x)$, $T(x,0) = T_0(x)$, where we now take $\Omega = (0,1)^d$ to be either two or three dimensional (i.e. $d = 2$ or $d = 3$). In contrast to Kobayashi's model, for which proving well-posedness is quite intricate (see for example [3]), this is relatively straightforward for the new model and essentially combines a Galerkin approach with a repeated use of the equivalence of relevant seminorms. The results are formulated in terms of Sobolev spaces $H^m_p(\Omega)$, $m \in \mathbb{N}$, of functions $f \in H^m_{loc}(\mathbb{R}^d)$ that are 1-periodic in all spatial directions. In the following, C denotes a generic constant that does not depend on the relevant quantities.

Theorem 3.1 (Existence and regularity of weak solutions)**.** *Let $\bar{t} > 0$ and suppose that*

$$(u_0, T_0) \in H^1_p(\Omega) \times H^1_p(\Omega).$$

Then, the above problem, defined via r-regular wavelets with $r \geq 2$, has a weak solution with

$$u \in L^\infty(0,\bar{t}; H^1_p(\Omega)) \cap L^2(0,\bar{t}; H^2_p(\Omega)),$$
$$T \in L^\infty(0,\bar{t}; H^1_p(\Omega)) \cap L^2(0,\bar{t}; H^2_p(\Omega))$$

and

$$u_t \in L^2(0,\bar{t}; L^2_p(\Omega)), \quad T_t \in L^2(0,\bar{t}; L^2_p(\Omega)).$$

Furthermore, if $(u_0, T_0) \in H^2_p(\Omega) \times H^2_p(\Omega)$, then

$$u, T \in H^1(0,\bar{t}; H^1_p(\Omega)),$$

and

$$u, T \in L^\infty(0,\bar{t}; H^2_p(\Omega)),$$

and thus also $u, T \in L^\infty(0,\bar{t}; L^\infty_p(\Omega))$.

Proof. In order to work with weak solutions, we introduce, as in reference [11], the bilinear form $\mathcal{B} : H^1_p(\Omega) \times H^1_p(\Omega) \to \mathbb{R}$ with

$$\mathcal{B}(u,v) = \lim_{n\to\infty} (\Delta_w u_n, v),$$

where $u, v \in H^1_p(\Omega)$ and (u_n) is a sequence of $H^2_p(\Omega)$ functions converging to u in the norm of $H^1_p(\Omega)$. It can be shown that the definition of $\mathcal{B}$ is independent of the

choice of the sequence (u_n). With this definition of $\mathcal{B}$, we state the following weak formulation of the problem:

$$(u_t, \varphi) = \varepsilon \mathcal{B}(u, \varphi) - \frac{1}{\varepsilon}(W_u(u; m), \varphi), \tag{13}$$

$$(T_t, \phi) = -c(\nabla T, \nabla \phi) + K(u_t, \phi) \quad \text{for all} \quad \varphi, \phi \in H^1_p(\Omega), \tag{14}$$

with

$$m(t) = \frac{c_1}{\pi} \arctan(c_2(T_e - T(t))),$$

and $c_1 < 1$.

For the Galerkin approximation we insert

$$u^n(x,t) = \sum_{j=0}^{n} b_j(t)\varphi_j(x), \qquad T^n(x,t) = \sum_{j=0}^{n} d_j(t)\varphi_j(x),$$

where the set $\{\varphi_j\}_j$ forms an orthonormal basis of $H^1_p(\Omega)$ (e.g., we can consider the smooth eigenfunctions of the Laplacian on the periodic torus). Then we consider the weak formulation above in terms of the basis functions, yielding

$$(u^n_t, \varphi_k) = \varepsilon \mathcal{B}(u^n, \varphi_k) - \frac{1}{\varepsilon}(W_u(u^n; m^n), \varphi_k), \tag{15}$$

$$(T^n_t, \varphi_k) = -c(\nabla T^n, \nabla \varphi_k) + K(u^n_t, \varphi_k), \tag{16}$$

$$(u^n, \varphi_k) = \xi_k, \tag{17}$$

$$(T^n, \varphi_k) = \eta_k, \quad k = 0, \dots, n, \tag{18}$$

with

$$m^n(t) = \frac{c_1}{\pi} \arctan(c_2(T_e - T^n(t))),$$

for $c_1 < 1$. Here $\xi_k = \xi_k(n)$ are such that

$$\sum_{j=0}^{n} \xi_j \varphi_j \to u_0 \ \text{ in } H^1_p(\Omega),$$

as $n \to \infty$, and for $\eta_k(n)$ as $n \to \infty$,

$$\sum_{j=0}^{n} \eta_j \varphi_j \to T_0 \text{ in } H^1_p(\Omega).$$

As the φ_j form a basis of the above spaces and as $u_0 \in H^1_p(\Omega)$, $T_0 \in H^1_p(\Omega)$, such coefficients do exist. Due to the orthogonality of the basis functions we obtain an ODE system for the coefficients whose system function is locally Lipschitz due to the boundedness of the bilinear form $\mathcal{B}$. This gives local existence.

We obtain bounds for the Galerkin approximation and then pass to the limit. Therefore we drop the superscript n from our notation and keep in mind that we are working with the finite-dimensional approximation until the limiting process is mentioned.

Testing equation (13) by u yields

$$\frac{1}{2}\frac{\mathrm{d}}{\mathrm{d}t}\|u\|^2 + \varepsilon |u|^2_B = -\frac{1}{\varepsilon}(W_u(u; m), u),$$

as we can use in the Galerkin approximation that $\mathcal{B}(u, u) = (\Delta_w u, u) = -|u|^2_B$ (see e.g. [11]).

The second term reads, noting that by the choice of $c_1 < 1$ we can use that $m \in [-\frac{1}{2}+\delta, \frac{1}{2}-\delta]$ for some small number $\delta \ll 1$,

$$-\frac{1}{\varepsilon}\int_\Omega W_u(u;m)u\,\mathrm{d}x \le \frac{1}{\varepsilon}\int_\Omega -u^4 + (2-\delta)u^2|u| + \left(m-\frac{1}{2}\right)u^2\,\mathrm{d}x \le \frac{1}{2\varepsilon}(-\|u\|^4 + 2\|u\|^2).$$

We have used that $(\int_\Omega u^2\,\mathrm{d}x)^2 \le \int_\Omega u^4\,\mathrm{d}x$. Hence if $\|u\| > \sqrt{2}$, then $\frac{\mathrm{d}}{\mathrm{d}t}\|u\| \le 0$, independently of the value of m (with more care one can derive a sharper bound). We have thus established the following uniform bound on the $L^2_p(\Omega)$ norm:

$$\|u\| \le \max\{\sqrt{2}, \|u_0\|\}.$$

Additionally, as $-\|u\|^4 + 2\|u\|^2 \le 1$, we get the following $\bar{t}$-dependent bound, after integrating over $[0,\bar{t}]$:

$$\frac{1}{2}\|u(\bar{t})\|^2 + \int_0^{\bar{t}} \varepsilon|u|_B^2\,\mathrm{d}t \le \frac{1}{2}\|u_0\|^2 + \frac{\bar{t}}{2\varepsilon}.$$

As the B seminorm is equivalent to the Besov $B^1_{2,2}(\Omega)$ seminorm for sufficiently regular wavelets, it is equivalent to the $H^1_p(\Omega)$ seminorm; see the discussions and references in the papers by Dobrosotskaya and Bertozzi [9, 11]. Thanks to this equivalence we obtain $\int_0^{\bar{t}} \varepsilon|u|^2_{H^1_p(\Omega)}\,\mathrm{d}t \le C + \bar{t}/(2\varepsilon)$, and hence we have, for any fixed $\bar{t}$,

$$u \in L^\infty(0,\bar{t}; L^2_p(\Omega)), \quad u \in L^2(0,\bar{t}; H^1_p(\Omega)).$$

Testing equation (13) with u_t gives

$$\|u_t\|^2 = -\frac{\varepsilon}{2}\frac{\mathrm{d}}{\mathrm{d}t}|u|_B^2 - \frac{1}{\varepsilon}(W_u(u;m), u_t). \tag{19}$$

Integrating over the time interval $[0,s]$, with $0 < s \le \bar{t}$, yields

$$\int_0^s \|u_t\|^2\,\mathrm{d}t + \frac{\varepsilon}{2}|u(s)|_B^2 = \frac{\varepsilon}{2}|u(0)|_B^2 - \frac{1}{\varepsilon}\int_0^s (W_u(u;m), u_t)\,\mathrm{d}t.$$

We control the last term on the right-hand side via

$$\begin{aligned}-\frac{1}{\varepsilon}\int_0^s (W_u(u;m), u_t)\,\mathrm{d}t &= \frac{1}{\varepsilon}\int_0^s\int_\Omega -u^3u_t + \left(\frac{3}{2}-m\right)u^2u_t + \left(m-\frac{1}{2}\right)uu_t\,\mathrm{d}x\,\mathrm{d}t \\ &\le -\frac{1}{4\varepsilon}\int_0^s \frac{\mathrm{d}}{\mathrm{d}t}\|u\|^4_{L^4_p(\Omega)}\,\mathrm{d}t + \frac{1}{\varepsilon}\int_0^s (2u^2+|u|, |u_t|)\,\mathrm{d}t,\end{aligned}$$

where we have used that $|m| \le 1/2$, which follows from (7) if $c_1 < 1$. Applying first the Cauchy–Schwarz inequality and then Young's inequality to the inner product underneath the last integral, we get

$$\begin{aligned}-\frac{1}{\varepsilon}\int_0^s (W_u(u;m), u_t)\,\mathrm{d}t \le &-\frac{1}{4\varepsilon}(\|u(s)\|^4_{L^4_p(\Omega)} - \|u(0)\|^4_{L^4_p(\Omega)}) \\ &+ \frac{1}{2\varepsilon^2}\int_0^s \|2u^2+|u|\|^2\,\mathrm{d}t + \frac{1}{2}\int_0^s \|u_t\|^2\,\mathrm{d}t.\end{aligned}$$

However, $\|2u^2+|u|\|^2 \le 8\|u^2\|^2 + 2\|u\|^2$; thus,

$$\begin{aligned}-\frac{1}{\varepsilon}\int_0^s (W_u(u;m), u_t)\,\mathrm{d}t \le &-\frac{1}{4\varepsilon}(\|u(s)\|^4_{L^4_p(\Omega)} - \|u(0)\|^4_{L^4(\Omega)}) + \frac{4}{\varepsilon^2}\int_0^s \|u\|^4_{L^4_p(\Omega)}\,\mathrm{d}t \\ &+ \frac{1}{2}\int_0^s \|u_t\|^2\,\mathrm{d}t + \frac{1}{\varepsilon^2}\int_0^s \|u\|^2\,\mathrm{d}t.\end{aligned}$$

Using the $L^2(\Omega)$ norm bound on u, inserting into (19) and rearranging yields

$$\frac{1}{2}\int_0^s \|u_t\|^2 \,\mathrm{d}t + \frac{\varepsilon}{2}|u(s)|_B^2 + \frac{1}{4\varepsilon}\|u(s)\|_{L^4_p(\Omega)}^4 \leq C(s) + \frac{4}{\varepsilon^2}\int_0^s \|u\|_{L^4_p(\Omega)}^4 \,\mathrm{d}t.$$

In particular we have, with $F(s) := \|u(s)\|_{L^4_p(\Omega)}^4$, the inequality

$$F(s) \leq C(s,\varepsilon) + \frac{16}{\varepsilon}\int_0^s F(t)\,\mathrm{d}t, \quad s \in (0,\bar{t}].$$

Gronwall's inequality then yields, as $C(s,\varepsilon)$ is nondecreasing in s (and therefore $C(s,\varepsilon) \leq C(\bar{t},\varepsilon)$, that

$$F(\bar{t}) \leq C(\bar{t},\varepsilon)\,\mathrm{e}^{\int_0^{\bar{t}} \frac{16}{\varepsilon}\,\mathrm{d}t} = C(\bar{t},\varepsilon)\,\mathrm{e}^{\frac{16\bar{t}}{\varepsilon}} = \tilde{C}(\bar{t},\varepsilon).$$

This bound grows exponentially fast with $\bar{t}$, but it does imply that, for $\bar{t} > 0$ fixed,

$$u \in L^\infty(0,\bar{t};L^4_p(\Omega)), \quad u_t \in L^2(0,\bar{t};L^2_p(\Omega)), \tag{20}$$

and thanks to the equivalence of the seminorm $|\cdot|_B$ to $|\cdot|_{H^1_p(\Omega)}$ we have $a|u(\bar{t})|_{H^1_p(\Omega)} \leq |u(\bar{t})|_B$, where a is a positive constant. We conclude further the bound

$$u \in L^\infty(0,\bar{t};H^1_p(\Omega)). \tag{21}$$

Now we establish bounds on the temperature. Testing (14) with T_t leads to

$$\|T_t\|^2 + \frac{c}{2}\frac{\mathrm{d}}{\mathrm{d}t}|T|^2_{H^1_p(\Omega)} = K(u_t,T_t) \leq \frac{K^2}{2}\|u_t\|^2 + \frac{1}{2}\|T_t\|^2. \tag{22}$$

Integrating over time yields, using (20),

$$\int_0^{\bar{t}} \|T_t\|^2 \,\mathrm{d}t + c|T(\bar{t})|^2_{H^1_p(\Omega)} \leq C(T(0),\bar{t},K) \tag{23}$$

and

$$T \in L^\infty(0,\bar{t};H^1_p(\Omega)), \quad T_t \in L^2(0,\bar{t};L^2_p(\Omega)).$$

To obtain a bound on higher-order Sobolev norms of u, we test with $-\Delta u$ and we obtain

$$\begin{aligned}
\frac{\mathrm{d}}{\mathrm{d}t}|u|^2_{H^1_p(\Omega)} &= \varepsilon(\Delta_w \nabla u, \nabla u) + \frac{1}{\varepsilon}\int_\Omega W_u(u;m)\Delta u \,\mathrm{d}x \\
&\leq -\varepsilon|\nabla u|_B^2 + C(\varepsilon,\bar{\varepsilon})\int_\Omega u^6 \,\mathrm{d}x + \frac{\varepsilon\bar{\varepsilon}}{2}|\nabla u|^2_{H^1_p(\Omega)} + C(\varepsilon,\bar{\varepsilon}) \\
&\leq -\tilde{C}|\nabla u|^2_{H^1_p(\Omega)} + C\|u\|^6_{H^1_p(\Omega)} + C(\varepsilon,\bar{\varepsilon}).
\end{aligned}$$

Here we have used a small $\bar{\varepsilon}$ to get rid of the second-order term with the wrong sign. As $u \in L^\infty(0,\bar{t};H^1_p(\Omega))$, we obtain by integration that

$$|u(\bar{t})|^2_{H^1_p(\Omega)} + C\int_0^{\bar{t}} \|\Delta u(t)\|^2 \,\mathrm{d}t \leq C\bar{t},$$

and we have the desired result $u \in L^2(0,\bar{t};H^2_p(\Omega))$.

Similarly we test the heat equation (12b) with $-\Delta T$ to deduce that

$$\frac{1}{2}\frac{\mathrm{d}}{\mathrm{d}t}|T|^2_{H^1_p(\Omega)} + c\|\Delta T\|^2 = -K(u_t,\Delta T) \leq C(K,c)\|u_t\|^2 + \frac{c}{2}\|\Delta T\|^2.$$

Using the bound on u_t and integrating gives that $T \in L^2(0,\bar{t};H^2_p(\Omega))$.

A usual limiting process (following e.g. [34], Chapter 3) yields global existence.

It remains to show that $u \in L^\infty(0,\bar{t};L^\infty_p(\Omega))$. We shall confine ourselves to the case of $d=3$ space dimensions; for $d=2$ the proof is simpler, as the embedding theorem used in the argument below is stronger for $d=2$ than for $d=3$.

Taking the inner product (on the Galerkin level throughout the rest of this proof) of the phase field equation with $-\Delta u_t$ yields that

$$(u_t,-\Delta u_t)+\varepsilon\mathcal{B}(u,-\Delta u_t)=-\frac{1}{\varepsilon}(W_u(u;m),-\Delta u_t).$$

Hence,

$$\|\nabla u_t\|^2+\frac{\varepsilon}{2}\frac{\mathrm{d}}{\mathrm{d}t}|\nabla u|_B^2=-\frac{1}{\varepsilon}\int_\Omega W_{uu}(u;m)\nabla u\cdot\nabla u_t+W_{um}(u;m)\nabla m\cdot\nabla u_t\,\mathrm{d}x,$$

which implies the inequality

$$\|\nabla u_t\|^2+\frac{\varepsilon}{2}\frac{\mathrm{d}}{\mathrm{d}t}|\nabla u|_B^2\le\frac{1}{\varepsilon}\int_\Omega |W_{uu}(u;m)\nabla u\cdot\nabla u_t|+|W_{um}(u;m)\nabla m\cdot\nabla u_t|\,\mathrm{d}x.$$

Since

$$W(u;m)=\frac{1}{4}u^2(u-1)^2+m\left(\frac{1}{3}u^3-\frac{1}{2}u^2\right)=\frac{1}{4}(u^4-2u^3+u^2)+m\left(\frac{1}{3}u^3-\frac{1}{2}u^2\right),$$

we have that

$$W_{uu}(u;m)=3u^2-3u+\frac{1}{2}+m(2u-1)$$

and

$$W_{um}(u;m)=u^2-u.$$

As $|m(T)|\le c_1/2$, it follows that

$$|W_{uu}(u;m)|\le C(u^2+1)\quad\text{and}\quad|W_{um}(u;m)|\le C(u^2+1).$$

Thus (with now C signifying a constant that may depend on ε and other constants in the statement of the problem, but is independent of u, m, T and the dimensions of the Galerkin subspaces from which u, m and T are picked),

$$\|\nabla u_t\|^2+\frac{\varepsilon}{2}\frac{\mathrm{d}}{\mathrm{d}t}|\nabla u|_B^2\le C\int_\Omega(u^2+1)|\nabla u|\,|\nabla u_t|\,\mathrm{d}x+C\int_\Omega(u^2+1)|\nabla m|\,|\nabla u_t|\,\mathrm{d}x.$$

Thanks to Hölder's inequality,

$$\begin{aligned}\|\nabla u_t\|^2+\frac{\varepsilon}{2}\frac{\mathrm{d}}{\mathrm{d}t}|\nabla u|_B^2\le{}&C\|u^2+1\|_{L^3_p(\Omega)}\|\nabla u\|_{L^6_p(\Omega)}\|\nabla u_t\|\\&+C\|u^2+1\|_{L^3_p(\Omega)}\|\nabla m\|_{L^6_p(\Omega)}\|\nabla u_t\|.\end{aligned}$$

By noting that $\|u^2+1\|_{L^3_p(\Omega)}\le C(\|u\|^2_{L^6_p(\Omega)}+1)$, $\|\nabla m\|_{L^6_p(\Omega)}\le C\|\nabla T\|_{L^6_p(\Omega)}$, and invoking the continuous embedding of the Sobolev space $H^1_p(\Omega)$ into $L^6_p(\Omega)$ (recall that, by hypothesis, $d=3$), we have that

$$\begin{aligned}\|\nabla u_t\|^2+\frac{\varepsilon}{2}\frac{\mathrm{d}}{\mathrm{d}t}|\nabla u|_B^2\le{}&C(\|u\|^2_{H^1_p(\Omega)}+1)\|\nabla u\|_{H^1_p(\Omega)}\|\nabla u_t\|\\&+C(\|u\|^2_{H^1_p(\Omega)}+1)\|\nabla T\|_{H^1_p(\Omega)}\|\nabla u_t\|.\end{aligned}$$

Hence, by Cauchy's inequality ($ab\le\frac{\eta}{2}a^2+\frac{1}{2\eta}b^2$ for any $a,b\ge0$ and $\eta>0$),

$$\frac{1}{2}\|\nabla u_t\|^2+\frac{\varepsilon}{2}\frac{\mathrm{d}}{\mathrm{d}t}|\nabla u|_B^2\le C(\|u\|^2_{H^1_p(\Omega)}+1)^2\left(\|\nabla u\|^2_{H^1_p(\Omega)}+\|\nabla T\|^2_{H^1_p(\Omega)}\right).\tag{24}$$

Now, thanks to eq. (6), upon taking the inner product with $-\Delta T_t$, we have that

$$\|\nabla T_t\|^2 + \frac{c}{2}\frac{\mathrm{d}}{\mathrm{d}t}\|\Delta T\|^2 = K(\nabla u_t, \nabla T_t).$$

Thus, again by Cauchy's inequality,

$$\frac{1}{2}\|\nabla T_t\|^2 + \frac{c}{2}\frac{\mathrm{d}}{\mathrm{d}t}\|\Delta T\|^2 \leq \frac{1}{2}K^2\|\nabla u_t\|.$$

Adding this last inequality to the inequality (24) multiplied by $2K^2$, we deduce that

$$\begin{aligned}\frac{1}{2}K^2\|\nabla u_t\|^2 + K^2\varepsilon\frac{\mathrm{d}}{\mathrm{d}t}|\nabla u|_B^2 + \frac{1}{2}\|\nabla T_t\|^2 + \frac{c}{2}\frac{\mathrm{d}}{\mathrm{d}t}\|\Delta T\|^2 \\ \leq C(\|u\|^2_{H^1_p(\Omega)} + 1)^2\big(\|\nabla u\|^2_{H^1_p(\Omega)} + \|\nabla T\|^2_{H^1_p(\Omega)}\big).\end{aligned} \tag{25}$$

Let us consider the terms appearing in the last pair of brackets in (25). We note that by Poincaré's inequality for a 1-periodic function $w \in H^1_p(\Omega)$ on $\Omega = (0,1)^3$, with integral average over Ω equal to zero, $\|w\|^2 \leq C|w|^2_{H^1_p(\Omega)}$. As each of the partial derivatives of u can be taken, in turn, as such a function w (note that by the divergence theorem $\int_\Omega \partial u/\partial x_i \,\mathrm{d}x = 0$, $i = 1,2,3$, thanks to the periodicity of u), we have that $\|\nabla u\|^2 \leq C|\nabla u|^2_{H^1_p(\Omega)}$, and therefore

$$\|\nabla u\|^2_{H^1_p(\Omega)} = \|\nabla u\|^2 + |\nabla u|^2_{H^1_p(\Omega)} \leq C|\nabla u|^2_{H^1_p(\Omega)}.$$

Consequently, by the norm equivalence $|\cdot|_{H^1_p(\Omega)} \sim |\cdot|_B$, it follows that

$$\|\nabla u\|^2_{H^1_p(\Omega)} \leq |\nabla u|^2_B. \tag{26}$$

Further, by the definition of the Sobolev norm $\|\cdot\|_{H^2_p(\Omega)}$ and the elliptic regularity estimate $\|T\|_{H^2_p(\Omega)} \leq C\|\Delta T\|$ for 1-periodic functions on Ω, we have that

$$\|\nabla T\|^2_{H^1_p(\Omega)} = \|\nabla T\|^2 + |\nabla T|^2_{H^1_p(\Omega)} \leq \|T\|^2_{H^2_p(\Omega)} \leq C\|\Delta T\|^2. \tag{27}$$

By substituting (26) and (27) into (25), we deduce that

$$\begin{aligned}\frac{1}{2}K^2\|\nabla u_t\|^2 + K^2\varepsilon\frac{\mathrm{d}}{\mathrm{d}t}|\nabla u|_B^2 + \frac{1}{2}\|\nabla T_t\|^2 + \frac{c}{2}\frac{\mathrm{d}}{\mathrm{d}t}\|\Delta T\|^2 \\ \leq C(\|u\|^2_{H^1_p(\Omega)} + 1)^2\big(|\nabla u|^2_B + \|\Delta T\|^2\big).\end{aligned}$$

Upon integration of this inequality with respect to the temporal variable, we have that, for any $t \in (0, \bar{t}]$,

$$\begin{aligned}&\frac{1}{2}\left(\int_0^t \left(K^2\|\nabla u_t(s)\|^2 + \|\nabla T_t(s)\|^2\right)\mathrm{d}s\right) + K^2\varepsilon|\nabla u(t)|^2_B + \frac{c}{2}\|\Delta T(t)\|^2 \\ &\quad\leq K^2\varepsilon|\nabla u(0)|^2_B + \frac{c}{2}\|\Delta T(0)\|^2 \\ &\qquad + C\int_0^t (\|u(s)\|^2_{H^1_p(\Omega)} + 1)^2\big(\|\nabla u(s)\|^2_B + \|\Delta T(s)\|^2\big)\,\mathrm{d}s.\end{aligned}$$

Let $c_0 := \min(K^2\varepsilon, \frac{c}{2})$ and $c_1 := \max(K^2\varepsilon, \frac{c}{2})$, and multiply the last inequality by $1/c_0$ to deduce that

$$\begin{aligned}\frac{1}{2c_0}\left(\int_0^t \left(K^2\|\nabla u_t(s)\|^2 + \|\nabla T_t(s)\|^2\right) \mathrm{d}s\right) + \left(|\nabla u(t)|_B^2 + \|\Delta T(t)\|^2\right)\\ \leq \frac{c_1}{c_0}\left(|\nabla u(0)|_B^2 + \|\Delta T(0)\|^2\right)\\ + \frac{C}{c_0}\int_0^t (\|u(s)\|_{H_p^1(\Omega)}^2 + 1)^2\left(\|\nabla u(s)\|_B^2 + \|\Delta T(s)\|^2\right) \mathrm{d}s \quad \forall t \in (0, \bar{t}].\end{aligned}$$

Thus, by Gronwall's inequality,

$$\begin{aligned}\frac{1}{2c_0}\left(\int_0^t \left(K^2\|\nabla u_t(s)\|^2 + \|\nabla T_t(s)\|^2\right) \mathrm{d}s\right) + \left(|\nabla u(t)|_B^2 + \|\Delta T(t)\|^2\right)\\ \leq \frac{c_1}{c_0}\left(|\nabla u(0)|_B^2 + \|\Delta T(0)\|^2\right) \exp\left(\frac{C}{c_0}\int_0^t (\|u(s)\|_{H_p^1(\Omega)}^2 + 1)^2 \,\mathrm{d}s\right) \quad \forall t \in (0, \bar{t}].\end{aligned}$$

As already established in (21), $u \in L^\infty(0, \bar{t}; H_p^1(\Omega))$, so it follows that the argument of the exponential appearing in the last inequality in bounded by a constant. Thus, in conjunction with norm equivalence and elliptic regularity, in precisely the same way as in (26) and (27) above, we deduce from the last inequality that

$$\begin{aligned}&u, T \in H^1(0, \bar{t}; H_p^1(\Omega)),\\ &u, T \in L^\infty(0, \bar{t}; H_p^2(\Omega)) \subset L^\infty(0, \bar{t}; L_p^\infty(\Omega)),\end{aligned}$$

provided that $u_0, T_0 \in H^2(\Omega)$. □

Theorem 3.2 (Uniqueness and continuous dependence on the initial data)**.** *The solutions from Theorem 3.1 are uniquely defined and depend continuously on the initial data u_0, T_0 in $H_p^2(\Omega)$, assuming that $d \leq 3$ and that the temperature stays below the melting temperature. In particular we then have, for all u_i^0, T_i^0, $i = 1, 2$, in $H_p^2(\Omega)$, that*

$$\|u_1 - u_2\|_{H_p^1(\Omega)}^2 + \|T_1 - T_2\|_{H_p^1(\Omega)}^2 \leq C\left[\|u_1^0 - u_2^0\|_{H_p^1(\Omega)}^2 + \|T_1^0 - T_2^0\|_{H_p^1(\Omega)}^2\right] \mathrm{e}^{Ct}. \quad (28)$$

Remark 1. The proof of the inequality (28) presented below relies on bounding u_i, $i = 1, 2$, in the $L^\infty(0, \bar{t}; L_p^\infty(\Omega))$ norm, which is deduced by bounding u_i, $i = 1, 2$, in the $L^\infty(0, \bar{t}; H_p^2(\Omega))$ norm and using the continuous embedding of $H_p^2(\Omega)$ into $L_p^\infty(\Omega)$ for $d \leq 3$. The derivation of the $L^\infty(0, \bar{t}; H_p^2(\Omega))$ norm bound on u_i, $i = 1, 2$, in turn rests on assuming that u_i^0, T_i^0, $i = 1, 2$, belong to $H_p^2(\Omega)$. In particular, the constant C appearing in (28) depends on the $H_p^2(\Omega)$ norms of u_i^0, T_i^0, $i = 1, 2$, even though the expression in the square bracket on the right-hand side of (28) only involves their $H_p^1(\Omega)$ norms.

Proof. We define two solutions (u_1, T_1), (u_2, T_2) and their difference $(w, v) = (u_1 - u_2, T_1 - T_2)$. That leads to the weak system

$$(w_t, \varphi) = \varepsilon(\Delta_w w, \varphi) - \frac{1}{\varepsilon}(W_u(u_1; m_1) - W_u(u_2; m_2), \varphi), \quad (29)$$

$$(v_t, \psi) = c(\Delta v, \psi) + K(w_t, \psi), \quad (30)$$

for all φ, ψ in $H^1_p(\Omega)$. Testing with $(\varphi, \psi) = (w, v)$ yields

$$\frac{1}{2}\frac{\mathrm{d}}{\mathrm{d}t}\|w\|^2 = -\varepsilon|w|_B^2 - \frac{1}{\varepsilon}(W_u(u_1; m_1) - W_u(u_2; m_2), u_1 - u_2), \tag{31}$$

$$\frac{1}{2}\frac{\mathrm{d}}{\mathrm{d}t}\|v\|^2 = -c\|\nabla v\|^2 + K(w_t, v). \tag{32}$$

Under the assumptions on the initial data, both u_1 and u_2 belong to $L^\infty(0, \bar{t}; L^\infty_p(\Omega))$. Then, for $m_i \in [-1/2 + \delta, 1/2 - \delta]$, the polynomials $W_u(u_i, m_i)$ are Lipschitz continuous and we can choose a suitable positive constant C such that

$$\frac{1}{2}\frac{\mathrm{d}}{\mathrm{d}t}\left(\|w\|^2 + \|v\|^2\right) + \varepsilon|w|_B^2 + c|v|^2_{H^1_p(\Omega)} \le C\|w\|^2 + K\int_\Omega w_t v \,\mathrm{d}x. \tag{33}$$

Testing the phase field equation with $\varphi = w_t$ and the temperature equation with $-\Delta v$ yields additionally

$$\|w_t\|^2 + \varepsilon\frac{\mathrm{d}}{\mathrm{d}t}|w|_B^2 = -\frac{1}{\varepsilon}\int_\Omega (W_u(u_1; m_1) - W_u(u_2; m_2))w_t \,\mathrm{d}x \le C\|w\|\|w_t\|,$$

$$C_1\frac{\mathrm{d}}{\mathrm{d}t}\|\nabla v\|^2 + C_2\|\Delta v\|^2 \le \frac{1}{4}\|w_t\|^2.$$

Adding these inequalities gives

$$\frac{1}{4}\|w_t\|^2 + \frac{\mathrm{d}}{\mathrm{d}t}\left[\varepsilon|w|_B^2 + C_1\|\nabla v\|^2\right] \le C\|w\|^2.$$

Together with the estimate (33) we then deduce that

$$\frac{1}{2}\frac{\mathrm{d}}{\mathrm{d}t}\left(\|w\|^2 + 2\varepsilon|w|_B^2 + \|v\|^2 + 2C_1\|\nabla v\|^2\right) + \varepsilon|w|_B^2 + c|v|^2_{H^1_p(\Omega)} \le C\|w\|^2 + \frac{K^2}{2}\|v\|^2.$$

An application of Gronwall's inequality thus yields

$$\|w\|^2 + 2\varepsilon|w|_B^2 + \|v\|^2 + 2C_1\|\nabla v\|^2 \le C\left[\|w^0\|^2 + |w^0|_B^2 + \|v^0\|^2_{H^1_p(\Omega)}\right]\mathrm{e}^{Ct}.$$

In particular we can use the equivalence of the Besov seminorm $|\cdot|_B$ to the Sobolev seminorm $|\cdot|_{H^1_p(\Omega)}$ and estimation of constants to deduce the assertion (28). □

Remark 2. In the proof we have used that the temperature stays below the melting temperature (slightly above is also permissible) and this assumption requires that the initial temperature profile is also below this value.

4. **Numerical methods and comparisons.** The simulations are carried out with a pseudospectral method for both equations, the classical model and its wavelet analogue. While the definition of Δ_w suggests a natural discretization in wavelet space, we use a Fourier spectral method for the discretization of T with 1-periodic Fourier modes in both spatial directions. In terms of these expansions, the system is written as the following system of ODEs:

$$\sum_{j=0}^{N}\sum_{k\in\mathbb{Z}_j^2}\sum_{\psi\in\Psi}(w_{j,k,\psi})_t\psi_{j,k} = \varepsilon\sum_{j=0}^{N}\sum_{k\in\mathbb{Z}_j^2}\sum_{\psi\in\Psi} -2^{2j}w_{j,k,\psi}\psi_{j,k} + \sum_{j=0}^{N}\sum_{k\in\mathbb{Z}_j^2}\sum_{\psi\in\Psi} c_{j,k,\psi}\psi_{j,k},$$

$$\sum_j(\hat{T}_j)_t\exp(ijx2\pi) = \sum_j -j^2 4\pi^2\hat{T}_j\exp(ijx2\pi) + K\sum_j(\hat{\xi}_j)_t\exp(ijx2\pi).$$

The coefficients $c_{j,k,\psi}$ are related to the cubic polynomial

$$\mathcal{W}_u(u; m) = u(1-u)\big(u - \tfrac{1}{2} + m\big)$$

by a stationary wavelet transform and the Fourier coefficients $\hat{\xi}_j$ are determined by transforming $\sum_{j=0}^{N}\sum_{k,\psi\in\Psi}(w_{j,k,\psi})_t\psi_{j,k}$ into discrete Fourier space. We discretize in time by a semi-implicit Euler scheme that treats the linear parts implicitly:

$$\frac{w^+_{j,k,\psi}-w_{j,k,\psi}}{\Delta t} = -2^{2j}w^+_{j,k,\psi} + c_{j,k,\psi}, \tag{34a}$$

$$\frac{\hat{T}^+_j-\hat{T}_j}{\Delta t} = -j^2 4\pi^2\hat{T}^+_j + K\hat{\xi}_j, \tag{34b}$$

where the superscript + indicates the new, updated coefficients. We employ convex splitting to ensure stability, which is also reflected in the update (see below). We update the wavelet coefficients first and then use the resulting approximation for u_t to calculate the coefficients $\hat{\xi}_j$. Also note that the coefficients $c_{j,k,\psi}$ in (34a) are evaluated by using the coefficients of the temperature approximations $\hat{T}_j$ at the old time level.

The update for the temperature is completely standard for spectral methods. For the order parameter, however, we shall provide additional details. The stationary wavelet transform yields four fields for the scaling function coefficients A, and H, V, D for the horizontal, vertical and diagonal wavelet coefficients, respectively. In MATLAB with the corresponding ordering, to calculate the wavelet Laplacian we multiply the jth scale by $2^{2(N-j)}$. For the jth coefficient level, let $R_j \in \{A_j, H_j, V_j, D_j\}$ be one of the coefficient arrays, and $R_{3,j}$ the same kind of coefficients for the cubic expression; then we update, with the convex splitting parameter C,

$$R^+_j = \frac{R_j + (\Delta t/\tau)(R_{3,j} + CR_j)}{1 + (\Delta t/\tau)(2^{2(N-j)}\varepsilon + C)}.$$

4.1. **Limiting case: Allen–Cahn model.** Before we investigate the evolution of the new model numerically and compare it with the classical recrystallization model, it is instructive to probe the models in a simpler setting, so we consider a special case where the models introduced in Section 2 reduce to scalar Allen–Cahn type equations. Specifically, we set the latent heat parameter $K = 0$ and let the initial temperature field to be uniformly equal to the equilibrium temperature $T(x, 0) = T_e$, where T_e is a nonnegative constant. Then, the temperature remains constant, $m = 0$, and the homogeneous free energy contribution is symmetric,

$$W(u) = \frac{1}{4}u^2(u-1)^2, \tag{35}$$

and Kobayashi's model (4)–(7) reduces the anisotropic Allen–Cahn equation

$$u_t = \varepsilon\left[\nabla\cdot\big(\gamma(\theta)\gamma'(\theta)\nabla^\perp u\big) + \nabla\cdot\big(\gamma(\theta)^2\nabla u\big)\right] - \frac{1}{\varepsilon}W'(u). \tag{36}$$

The new model (12) with (4), (7) reduces to the "wavelet Allen–Cahn equation",

$$u_t = \varepsilon\Delta_w u - \frac{1}{\varepsilon}W'(u). \tag{37}$$

The above are $L^2_p(\Omega)$ gradient flows of the free energy (8), with $\zeta = H^1_p(\Omega)$ for the isotropic Allen–Cahn model, $\zeta = A$ for the anisotropic Allen–Cahn model, and $\zeta = B$ for the wavelet Allen–Cahn equation. For all numerical results in this section, the initial condition for u was a small uniformly distributed random perturbation of $u = 1$.

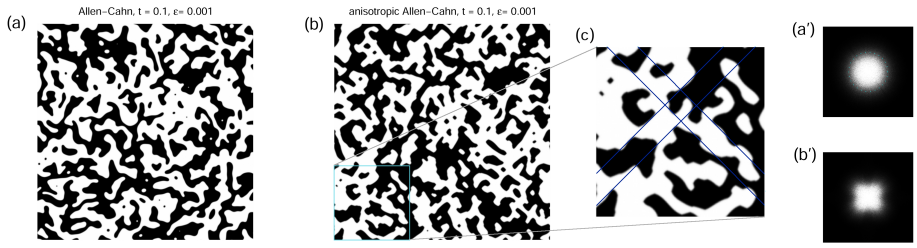

FIGURE 1. Panel (a) shows the numerical results for the isotropic Allen–Cahn model ((36) with $\delta = 0$) for $\varepsilon = 0.001$ on a 1024×1024 grid at $t = 0.1$, and (a') shows the absolute values of the corresponding two-dimensional discrete Fourier transform. In panel (b), we see the numerical results for the anisotropic Allen–Cahn model (36) with $\delta = 0.065$, with the same grid and values for t and ε. Again, panel (b') shows the absolute values of the corresponding Fourier transform. The zoom (c) highlights anisotropic features of the pattern in (b) in the spatial domain.

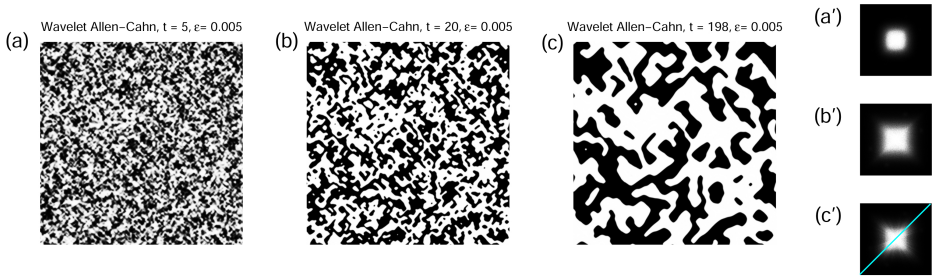

FIGURE 2. Numerical results for the wavelet-Allen–Cahn model (37) for $\varepsilon = 0.005$ on a 1024×1024 grid in a unit square at three different times. Panels (a'), (b') and (c') show the absolute values of the corresponding two-dimensional discrete Fourier transform.

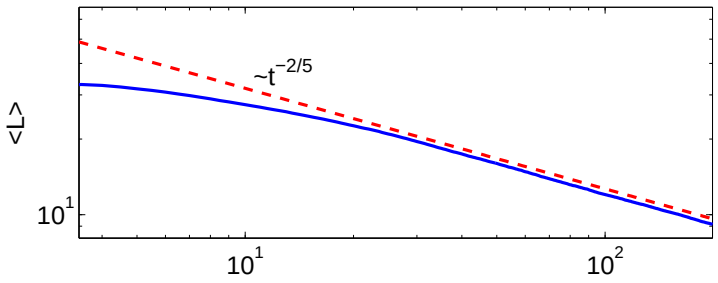

FIGURE 3. Coarsening diagram for the wavelet-Allen–Cahn equation, using the same parameters as in Figure 2. The figure shows the average length scale $\langle L \rangle$, versus t as a solid line, where $\langle L \rangle$ is defined in (38).

In Figure 1 we observe the well-known emergence of a coarsening pattern for the Allen–Cahn equation, which evolves isotropically as can be seen from the radial symmetry of the Fourier spectrum (a'), We also show the evolution for the anisotropic Allen–Cahn equation for $n = 4$ and $\delta = 0.065$, where the anisotropy is still in the weak regime. The resulting patterns show a directional dependence that is in accordance with a four-fold symmetry for γ, which is also reflected in the characteristic shape of the Fourier spectrum (b').

We now carry out a numerical study to investigate the emergence of anisotropy and its long-time evolution in the wavelet-Allen–Cahn equation. As has been shown in [10], volume constrained minimizers of the free energy using the Besov seminorm lead to Wulff shapes with a clear four-fold symmetry for the new wavelet-Allen–Cahn equation. Figures 2 (a)–(c) depict a typical evolution that compares well to the numerical results for the anisotropic Allen–Cahn equation (36). The white and black regions correspond to the order parameter being approximately 0 or 1. Coarsening takes place in a similar fashion as for the classical anisotropic Allen–Cahn model. Figures (a')–(c') show the absolute values of the Fourier transforms corresponding to the patterns in Figures (a)–(c). One clearly sees the emergence of an anisotropic pattern with a four-fold symmetry. Having said this, we emphasize that the observed similarities are merely qualitative; in particular, the time scales for the two sets of simulations are different ($t = 0.1$ for the classical model and $t = 5, 20, 198$ for wavelet-based model); the corresponding values of ε are also different ($\varepsilon = 0.001$ for the classical model and $\varepsilon = 0.005$ for the wavelet-based model). We have not, so far, made any attempts to calibrate the wavelet-based model so as to ensure that spatial and temporal scales quantitatively match those in the classical model.

In Figure 3 we show a coarsening diagram for the wavelet Allen–Cahn equation in a doubly logarithmic plot, for the same parameters as in Figure 2. For each line i of grid points parallel to the x-axis, we counted the number of domains $N_i(t)$ and averaged the N_i over all these lines, which gives a measure $\langle L\rangle$ for the inverse of the typical domain size:

$$\langle L\rangle = \frac{1}{n_y}\sum_{i=1}^{n_y} N_i(t). \tag{38}$$

The numerical results show that the coarsening rate approaches a power law behaviour $\langle L\rangle \sim t^{-2/5}$ for the isotropic Allen–Cahn equation and also for the wavelet Allen–Cahn equation as $t \to \infty$. Only the latter is shown in Figure 2.

4.2. **Recrystallization with thermal coupling.** While for the wavelet-Allen–Cahn case we have used small scaled uniformly distributed random noise as initial datum, here we instead insert a very narrow Gaussian into the domain as a nucleation site to start the recrystallization process, similarly to what happens in physical experiments. For comparison we note first a recent study [1] on numerical methods and conditions regarding the accurate numerical description of dendritic patterns. For our numerical implementation of the original model by Kobayashi, we consider the system (5) and (6) with

$$\gamma(\theta) = 1 + \delta\cos(4(\theta + \pi/6)). \tag{39}$$

Figures 4 and 5 show that the growing nucleus develops a branching structure with both models. In Figure 4 the branches are seen to align more closely with two mutually orthogonal directions, reflecting the four-fold symmetry imposed in

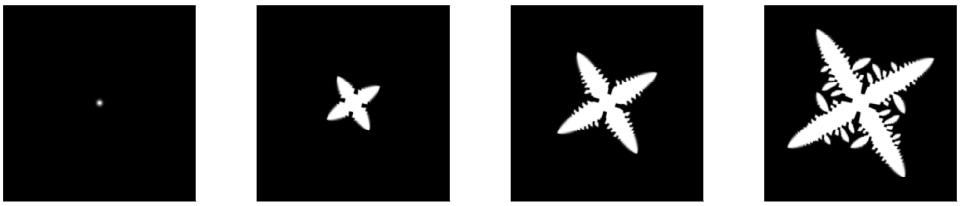

FIGURE 4. Numerical results for Kobayashi's model, (5) and (6), using γ as in (39) with $\delta = 0.15$.

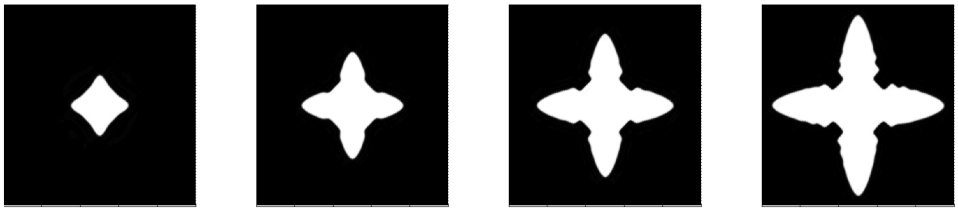

FIGURE 5. Dendritic growth based on the intrinsic anisotropy of the wavelet-Laplacian.

the Kobayashi model by γ. For the wavelet-based model the results are shown in Figure 5. The initial Gaussian nucleus exhibits faster growth in four preferred directions, which are now aligned with the co-ordinate axes. We also observe the onset of side-branching. As in the case of the numerical experiments presented in the previous subsection, we emphasize that the observed similarities between the results obtained with the two models are merely qualitative, and we have not, so far, made any attempts to calibrate the wavelet-based model so as to ensure that spatial and temporal scales quantitatively match those of the Kobayashi model.

5. **Conclusions and outlook.** This work explores the possibility of using the anisotropic nature of a wavelet analogue for a differential operator to construct mathematical models that describe anisotropic pattern formation in material science. For a standard model of dendritic crystal growth, we have demonstrated that simply replacing the H^1 seminorm representation for the interface contribution to the underlying free energy by a wavelet-based Besov seminorm produces an L^2 gradient flow with preferred growth directions that have four-fold symmetry. A wavelet Laplacian appears in the equation instead of the usual Laplacian.

Kobayashi's original model requires an explicit dependence of the surface tension coefficient on the phase field gradient to obtain anisotropy, thus leading to a quasi-linear PDE for the phase-field. In contrast, the wavelet-based approach uses a linear and derivative-free operator with an intrinsic anisotropy. Our results confirm that the evolution of the phase field for the new model exhibits anisotropy with four-fold symmetry, as suggested in [10] for the Allen–Cahn equation. Also, the coarsening rates compare well with those seen for the classical models.

Moreover, the new formulation lends itself naturally to numerical solutions via wavelet or hybrid e.g. wavelet-spectral methods. The fully discrete scheme uses convex splitting where the implicit terms are linear and is easily implemented in MATLAB with the help of the available wavelet tools.

We also note that the model is easily generalized to 3D and in fact our well-posedness result applies also to this case. It would be interesting to see if an efficient 3D implementation is possible that would be competitive with existing simulations using classical PDE models.

An issue that has been intensively discussed in connection with phase field models like Kobayashi's is the question whether these are formulated in a thermodynamically consistent way, see for example Caginalp [5], Penrose and Fife [25, 26], Wang et al. [31] and in the anisotropic case by McFadden et al. [22]. The focus of our paper has been to derive a wavelet-based analogue for one of the simplest models of dendritic growth. Concerning thermodynamical consistency of wavelet-based recrystallization models we remark that the coupled energy and phase-field equations are obtained via

$$\tau u_t = -\frac{\delta \mathcal{E}}{\delta u} = \varepsilon \Delta_w u - \frac{1}{\varepsilon} W_u(u;m),$$
$$e_t = -\nabla \cdot \left(M \nabla \frac{\delta}{\delta e} \int_\Omega \frac{e}{T}\, \mathrm{d}x \right) = -\nabla \cdot \left(M \nabla \frac{1}{T} \right) = \nabla \cdot \left(\frac{M}{T^2} \nabla T \right),$$

where $\mathcal{E}$ is the energy functional (8) with the wavelet seminorm, i.e. $\zeta = B$, and e is the internal energy density, $e = T + K(1-u)$. By setting $M = cT^2$, we deduce (12). We recall that in the "classical" context, thermodynamical consistency requires a relation between e and W, namely (cf. [23, 31]),

$$\frac{\partial (W/T)}{\partial (1/T)} = e.$$

Upon extending our models and analysis to these situations it will be interesting to discuss whether thermodynamical consistency with respect to a corresponding wavelet-based entropy remains a useful concept, and this is subject to further investigations.

There are, of course, a number of other open problems and directions for future research, such as extending our investigations to anisotropic surface energies with other symmetries. This may require using generalizations of wavelets such as shearlets, for example.

Acknowledgments. The authors thank Andrea Bertozzi for helpful comments and Dirk Peschka for sharing his valuable insight into anisotropic phase separation.

REFERENCES

[1] J. W. Barrett, H. Garcke, and R. Nürnberg. Stable Phase Field Approximations of Anisotropic Solidification. *IMA J. Numer. Anal.*, 34(4):1289–1327, 2014.
[2] A. Braides. *Gamma-Convergence for Beginners*. Oxford University Press, 2002.
[3] E. Burman and J. Rappaz. Existence of solutions to an anisotropic phase-field model. *Math. Meth. Appl. Sci.*, 26:1137–1160, 2003.
[4] W. K. Burton, N. Cabrera, and F. C. Frank. The Growth of Crystals and the Equilibrium Structure of their Surfaces. *Phil. Trans. R. Soc. Lond. A*, 243(866):299–358, 1951.
[5] G. Caginalp. Penrose–Fife modification of solidification equations has no freezing or melting. *Appl. Math. Lett.*, 5(2):93–96, 1992.
[6] C. Cattani. Harmonic wavelets towards the solution of nonlinear PDE. *Comp. Math. Appl.*, 50(8-9):1191–1210, 2005.

[7] W. Dahmen. Wavelet and Multiscale Methods for Operator Equations. *Acta Num.*, 6:55–228, 1997.
[8] I. Daubechies. *Ten lectures on wavelets*. SIAM, Philadelphia, PA, USA, 1992.
[9] J. A. Dobrosotskaya and A. L. Bertozzi. A Wavelet-Laplace Variational Technique for Image Deconvolution and Inpainting. *IEEE Trans. Imag. Proc.*, 17(5):657–663, 2008.
[10] J. A. Dobrosotskaya and A. L. Bertozzi. Wavelet analogue of the Ginzburg–Landau energy and its Gamma-convergence. *Interf. Free Boundaries*, 12(2):497–525, 2010.
[11] J. A. Dobrosotskaya and A. L. Bertozzi. Analysis of the Wavelet Ginzburg–Landau Energy in Image Applications with Edges. *SIAM J. Imaging Sci.*, 6(1):698–729, 2013.
[12] M. E. Glicksman. *Principles of Solidification*. Springer, 2011.
[13] C. Herring. Some theorems on the free energies of crystal surfaces. *Phys. Rev.*, 82(1):87–93, 1951.
[14] M. Holmström. Solving Hyperbolic PDEs Using Interpolating Wavelets. *SIAM J. Sci. Comput.*, 21(2):405–420, 1999.
[15] M. Holmström and J. Waldén. Adaptive Wavelet Methods for Hyperbolic PDEs. *J Sci. Comp.*, 13(1):19–49, 1998.
[16] L. Jameson. A Wavelet-Optimized, Very High Order Adaptive Grid and Order Numerical Method. *SIAM J. Sci. Comput.*, 19(6):1980–2013, 1998.
[17] A. Karma and W.-J. Rappel. Numerical Simulation of Three-Dimensional Dendritic Growth. *Phys. Rev. Lett.*, 77(19):4050, 1996.
[18] R. Kobayashi. Modeling and numerical simulations of dendritic crystal growth. *Physica D*, 63, 1993.
[19] B. Li, J. Lowengrub, A. Rätz, and A. Voigt. Geometric evolution laws for thin crystalline films: modeling and numerics. *Commun. Comput. Phys.*, 6:433–482, 2009.
[20] S. Mallat. *A Wavelet Tour of Signal Processing, Third Edition: The Sparse Way*. Academic Press, 2008.
[21] G. B. McFadden. Phase-field models of solidification. In *Recent Advances in Numerical Methods for Partial Differential Equations and Applications*, number 306 in Contemporary Mathematics, pages 107–145. American Mathematical Society, 2002.
[22] G. B. McFadden, A. A. Wheeler, R. J. Braun, S. R. Coriell, and R. F. Sekerka. Phase-field models for anisotropic interfaces. *Phys. Rev. E*, 48:2016–2024, 1993.
[23] A. Miranville. Some mathematical models in phase transitions. *DCDS-S*, 7:271–306, 2014.
[24] L. Modica. The gradient theory of phase transitions and the minimal interface criterion. *Arch. Rat. Mech. Anal.*, 98(2):123–142, 1987.
[25] O. Penrose and P. C. Fife. Thermodynamically consistent models of phase-field type for the kinetics of phase transitions. *Physica D*, 43:44–62, 1990.
[26] O. Penrose and P. C. Fife. On the relation between the standard phase-field model and a "thermodynamically consistent" phase field model. *Physica D*, 69:107–113, 1993.
[27] K. Schneider and O. V. Vasilyev. Wavelet Methods in Computational Fluid Dynamics. *Ann. Rev. Fluid Mech.*, 42(1):473–503, 2010.
[28] I. Steinbach. Phase-field models in materials science. *Mod. Sim. Mater. Sci. Eng*, 17(7):073001, 2009.
[29] O. V. Vasilyev and S. Paolucci. A Fast Adaptive Wavelet Collocation Algorithm for Multidimensional PDEs. *J. Comp. Phys.*, 138:16–56, 1997.
[30] O. V. Vasilyev, S. Paolucci, and M. Sen. A Multilevel Wavelet Collocation Method for Solving Partial Differential Equations in a Finite Domain. *J. Comp. Phys.*, 120:33–47, 1995.
[31] S.-L. Wang, R. F. Sekerka, A. A. Wheeler, B. T. Murray, S. R. Coriell, R. J. Braun, and G. B. McFadden. Thermodynamically-consistent phase-field models for solidification. *Physica D*, 69:189–200, 1993.
[32] A. A. Wheeler, B. T. Murray, and R. J. Schaefer. Computation of dendrites using a phase field model. *Physica D*, 66(243), 1993.
[33] G. Wulff. Zur Frage der Geschwindigkeit des Wachstums und der Auflösung der Krystallflächen. *Zeitschrift f. Krystall. Mineral.*, 34:449–530, 1901.
[34] S.-M. Zheng. *Nonlinear Evolution Equations*. Pitman series Monographs and Survey in Pure and Applied Mathematics 133, Chapman Hall/CRC, Boca Raton, Florida, 2004.

E-mail address: maciek.korzec@gmail.com
E-mail address: muench@maths.ox.ac.uk
E-mail address: suli@maths.ox.ac.uk
E-mail address: bwagner@math.tu-berlin.de